Turbulence Measurements in Subsonic and Supersonic Axisymmetric Jets in a Parallel Stream

Philip J. Morris*
Lockheed-Georgia Company, Marietta, Ga.

Measurements of mean and fluctuating velocity components have been made in an unheated axisymmetric jet mounted in a low-speed wind tunnel. The measurements were made with a backscatter laser velocimeter. Velocity measurements are presented for jet exit Mach number from 0.47 to 1.67 and tunnel velocity to jet exit velocity ratios from 0.1 to 0.5. The rate of growth of the annular mixing region agreed closely with that of the two-dimensional mixing layer. The potential core length was found to be nearly inversely proportional to the jet exit, freestream velocity difference. Peak axial turbulence intensities varied as the seven-tenths power of the velocity difference. The mean velocity, turbulence intensity and axial velocity skewness, and kurtosis distributions were found to agree with measurements of jets into still air using an appropriate local radial coordinate based on vorticity thickness.

I. Introduction

THE effect of a moving freestream on the development of an axisymmetric jet is currently of considerable importance, particularly in the field of aeroacoustics. This interest has been stimulated by discrepancies between noise measurements in simulated flight conditions, such as anechoic free jets, and wind tunnels, and flight test noise data. To properly predict the flyover noise from either simulated flight tests or static tests, it is essential to know how the jet noise sources alter in flight. These changes are reflected in alterations in the turbulent structure of the jet. Although a detailed description of the statistical properties of the turbulence is required to exactly describe the aerodynamic noise sources, scaling laws for overall radiation may be obtained from measurements of a few simple properties of the flow. In spite of this, there have been very few investigations of the mixing of two streams of finite velocity. Previous measurements of turbulence in jets in moving streams have rarely been at high speeds and have tended to ignore the initial mixing region of the jet, which is of particular importance in aeroacoustics. The turbulence measurements detailed in this paper provide much of this essential, missing information.

The measurement of the mean properties of a turbulent flow has a practical importance, but it is only by measuring the fluctuating components of the flow that it is possible to obtain a better understanding of the structure of the turbulent flow and provide justification for any mathematical hypotheses used in representing the motion. Measurements of the time-averaged properties of the flow may be achieved by total and static pressure surveys in high velocity and temperature flows. However, measurements of turbulent fluctuations have normally been limited to fairly low-speed flows, since in these velocity regions the conventional measuring devices, the hot-wire or hot-film anemometer, give uncontaminated velocity measurements and are structurally sound. It is only with the development of optical measurement techniques that accurate measurements have been viable in hot or high-speed turbulent flows. There are two main advantages in using optical techniques. Firstly, there is no need to insert a probe in the flow, which might disturb the flow regime or be physically incapable of withstanding stresses exerted by the flow. Secondly, an unambiguous measurement of velocity is obtained and measurements can be carried out in regions where the density and temperature may fluctuate.

There have been few experimental investigations of the mixing of two streams of finite velocity. The two-dimensional mixing layer is perhaps the simplest two-stream flow. Convenient similarity solutions for the mean velocity have been obtained using an eddy viscosity assumption, and this has led to several experimental investigations. Yule[1] made measurements of three components of mean and fluctuating velocity, shear stress, and longitudinal and lateral space correlations. The spreading parameter, σ, defined by Görtler[2] was found to vary with velocity ratio, λ, in the same manner as that found by Miles and Shih[3] and was given by

$$\sigma/\sigma_0 = (1-\lambda)/(1+\lambda)^{1/2} \tag{1}$$

where σ_0 is the value of σ for $\lambda=0$. λ is given by $\lambda=\bar{u}_T/\bar{u}_a$, where $\bar{u}_T$ is the tunnel velocity and $\bar{u}_a$ is the jet centerline velocity. It should be noted that Sabin[4] and Brown and Roshko[5] suggested a relationship of the form

$$\sigma/\sigma_0 = (1-\lambda)/(1+\lambda) \tag{2}$$

Brown and Roshko[5] made velocity and density measurements in mixing layers using gases of different densities, which permitted the effects of velocity ratio and density ratio to be examined separately.

Studies of round jets in moving streams have been made by Antonia and Bilger[6] and Forstall and Shapiro[7] among others. The former study examined the flow far downstream of the jet exit to determine whether assumptions of turbulence similarity could be made. The latter study considered low-speed jets with velocity ratios from 0.2 to 0.75. Mean velocity profiles were found to be similar in terms of a local radial coordinate based on the half-velocity radius, and the potential core length, x_c, varied with velocity ratio as

$$x_c/r_J = 8+24\lambda \tag{3}$$

where r_J is the jet exit radius.

Several points emerge from these and other previous experimental studies. Because of the relative ease of

Presented as Paper 76-25 at the AIAA 14th Aerospace Sciences Meeting, Washington, D. C., Jan. 26-28, 1976; submitted March 4, 1976; revision received May 17, 1976. This study was sponsored by NASA-Lewis under Contract NAS3-18540. The laser velocimeter system used in the experiments was developed at Lockheed-Georgia with funding from AFAPL/DOT under Contract F33615-73-C2032 and Lockheed-Georgia Company. The author wishes to acknowledge the help of C. B. Reid, P. D. Dean, R. H. Burrin, and H. E. Plumblee for their help in making the measurements.

Index categories: Jets, Wakes, and Viscid-Inviscid Flow Interactions.

*Research/Design and Development Engineer-Associate. Member AIAA.

measurement, the mean axial velocity is the most often measured quantity. Measurements of turbulence intensity have been made in relatively few experiments, and these have been limited by available instrumentation to low velocities. The main interest in round jets in moving streams appears to have been concentrated in two distinct areas. First, the rate of the decay of the jet centerline axial mean velocity has been studied. Second, the assumptions of similarity and self-preservation have been examined. This has, for the most part, involved measurements downstream of the end of the potential core. Clearly, the following areas are in need of attention: a) the effects of the secondary stream on the initial development of a round jet, b) the variation of turbulence intensity with velocity ratio, and c) the variation of turbulence intensity with jet Mach number.

The progress made toward understanding in these areas is described in the subsequent section. In Sec. II, the experimental facilities are described.

II. Experimental Facilities

A closed-circuit, single return, low-speed wind tunnel was used in the experiments. The test section was approximately 30×43 in. with a length of 48 in. The tunnel provided an empty flow velocity capability 0 to 310 fps. An 8-in. diam air duct was installed to supply air to the 2-in.-diam nozzles that exhausted axially down the center of the wind tunnel working section. The plenum pylon mount was faired with a 21% thick zero lift airfoil section. The 8-in. plenum was faired with a wooden bullet. An 8-in. to 4-in. reduction was attached to this plenum and smoothly faired to the end of a short length of 4-in. pipe, to which the nozzles were attached. A 9-in. spacer could be inserted upstream of the nozzle so that 17 diam of the jet flow could be viewed by the laser velocimeter through a glass working-section wall. The laser velocimeter was mounted on lead-screw and way systems on a hydraulic table outside the wind tunnel, which allowed three-dimensional traversing of the system. Slots in the wind tunnel wall just downstream of the working section were provided to vent the working section to ambient. A remotely operated door in the return section of the wind tunnel, which prevented pressure buildip in the tunnel, could be adjusted to obtain ambient static pressure in the working section. A sketch of the working section geometry is shown in Fig. 1.

There are a number of optical techniques for remotely detecting the velocity of particles in a flow. The approach described here is based on an interference pattern of light formed in the measurement volume by the intersection of two coherent monochromatic light beams. As a microscopie particle passes through this fringe pattern, light is scattered and detected by a photosensor. The detector output burst has a frequency dependent of the spacing of the interference pattern and the velocity component of the particle normal to the fringes. Since the fringe spacing is set by the geometry of the optics, the normal particle velocity is readily derived from the detector signal frequency. A system using this operating principle is called a "burst counter" laser velocimeter. A detailed account of much of the optics, electronics, and data processing used in the current laser velocimeter system is given in Refs. 8 and 9. However, a brief description of the configuration used in these experiments and some modifications that have been made are described here.

The laser velocimeter optical configuration is shown in Fig. 2. A 4-W Argon laser and a beam splitter/color separator assembly generated two pairs of blue, 4880 Å, and green, 5145 Å, beams. These beams were simultaneously focused and caused to cross by the transmitting lens. This created two coincident ellipsoidal measurement volumes of orthogonal green and blue fringe patterns. The dimensions of the $1/e^2$ measurement volume were nominally 0.3 mm by 2.0 mm with a total of 33 fringes. Light scattered by particles passing through the measurement volume was collected by receiving optics, mounted beside the transmission optics, and fed to a

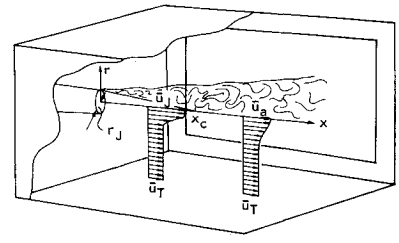

Fig. 1 Tunnel working section geometry.

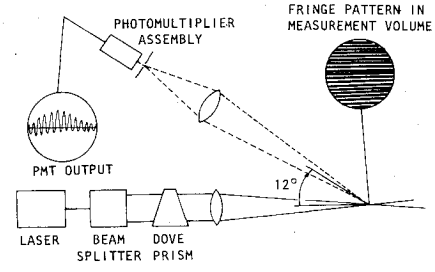

Fig. 2 Laser velocimeter optical system.

photomultiplier assembly. This assembly filtered the collected backscatter light into blue and green components, which were sensed by two photomultiplier tubes. The resulting electronic signal was fed to the digital processing unit and a computer to obtain the particle velocity. The jet air was seeded by introducing 1μ aluminum oxide particles, coated with CAB-O-SIL to reduce agglomeration, into the jet plenum. The wind tunnel flow was seeded using an aerosol of 1010 hydraulic oil generated Laskin nozzle. This generator, which was based on the design of Yanta[10] produced a particle size distribution that peaked at 1μ.

In the original optical configuration, with a pair of orthogonal fringe patterns at $\pm 45°$ to the jet axis, the laser velocimeter was able to provide measurements of two orthogonal components of velocity as long as the deviation of the instantaneous velocity vector from the axial direction was sufficiently small. This restriction is imposed since, in order to resolve the measured velocities into their axial and radial components, coincidence (simultaneous detection from both fringe patterns) is required. This results in a very small "angular window." The "angular window" may be defined as the maximum angle to the jet axis beyond which the particle has less than a certain high probability of simultaneous detection by light scattered from both color fringe patterns. For stationary fringes, this window is a function of measurement volume size and fringe spacing. Since this angular criterion is unlikely to be met in a turbulent jet flow, where the instantaneous velocity vector deviates significantly from the axial direction, these fringes were rotated 45° for the current measurements, and only the set of fringes normal to the jet axis were used. This meant that measurements of axial velocity only were made. This angular restriction can be alleviated by movement of the fringes within the measurement volume. This may be achieved by use of Bragg cell in the beam splitter optics, which frequency shifts one of a pair of one color light beams with respect to the other.

A most important aspect of the electronic processor is the data validation circuitry. The original design, described in Ref. 8, was based on a digital comparison of the time for the first four fringe crossings with the time for the second four, as well as an odd ratio, three to five. This comparison eliminated most erroneous data due to multiple particles in the measurement volume or an incorrect fringe crossing count. Because of the digital nature of the comparison, the acceptable time difference varied up to 3% of the period, and at higher frequencies (velocities), where the fringe crossing period was very small, the accepted error was an increasing

percentage of the period. This error window was found to be unacceptable for turbulence measurements at high speeds. A new circuit was constructed that still compared the same fringe crossing ratios but used an analog integrator. The error window was then constant at ±1% over a variable velocity range of 30 to 1. This system was used in the measurement program.

At the time that a measurement was taken, a magnetic tape was written that recorded each individual velocity and its time of occurrence. Before analyzing the data, it was necessary to process this recorded data to correct for the natural biasing of the velocity data. The amount of fluid passing through the measurement volume is proportional to the local fluid velocity, so that even if particles are uniformly distributed in the fluid, a bias toward higher velocities will occur, since in a finite number of velocity measurements, a higher proportion occur at the higher velocities. It can be shown[11] in a one-dimensional, unsteady flow that, if there is no dependence between the particle velocity and the particle density (uniform seeding), then the true mean velocity can be found by taking the reciprocal of the arithmetic mean of the particle periods (time for a particle to cross eight fringes) multiplied by a constant of proportionality. It can also be shown that this biasing effect leads to a weighting of the velocity probability distribution function that is proportional to the velocity. Since only one component of velocity was measured in these experiments, an instantaneous measurement of the vector velocity, which would be required for a complete unbiasing of the data in a three-dimensional flow, was not possible. Thus, a first-order correction of the data was obtained by using the instantaneous axial velocity for the vector velocity. The velocity probability distribution could then be corrected by multiplying the inverse of the velocity. The moments of the corrected distribution function were calculated giving the mean, standard deviation, skewness, and kurtosis. This bias correction is equivalent to that proposed by McLaughlin and Tiederman.[12]

A "burst counter" laser velocimeter system requires a high rate of seeding to obtain good spectral information. The data analysis procedure is described in Ref. 9. No frequency spectra were obtained in the present measurements, although the validated particle rate varied from 1,000 to 10,000 particles per second which, because of the use of random-time sampling and single particle detection, can provide frequency information up to 20 kHz.[9] In order to obtain satisfactory particle rate and distribution, the flow must be seeded artifically. The amplitude and phase response of the 1μ particles used in these experiments have been calculated in Ref. 8. At 10 kHz the particle velocity amplitude is 75% of the flow velocity and the pase lag is 40°. However, the frequency measured by the LV is higher than that seen by the particle traveling with the flow due to the upward Doppler shift for the stationary reference frame. This phenomenon reduces the particle response requirements by significant factors.

III. Experimental Program and Preliminary Measurements

The test conditions were designed to provide the maximum amount of useful data within the limits of the facility and instrumentation. The effects of two major changes were of interest. First, how does the secondary stream velocity affect the jet development at fixed jet exit velocity, and second, how does the jet exit Mach number affect the jet development? Thus, the experiments were divided into two sections. In the first, the jet exit velocity was held constant and the wind tunnel velocity varied. In the second, the jet exit Mach number was changed and the velocity ratio was kept constant. The first series of measurements were carried out at $M_J = 0.47$ and nominal velocity ratios of 0.1, 0.2, 0.3, 0.4, and 0.5. The second series of measurements were performed at a fixed velocity ratio of 0.1 and jet exit Mach numbers of 0.47, 0.9, 1.37, and 1.67. The jet air was unheated in all the experiments.

It was anticipated that the general effect of increasing both velocity ratio and Mach number would be to stretch the jet flow in the axial direction. In order to obtain a representative set of turbulence measurements in the first series ($M_J = 0.47$ for various velocity ratios), the following procedure was adopted. First, a jet centerline traverse was carried out to give an indication of the potential core length, x_c. Radial traverses were then performed at axial locations close to x_c, $x_c/2$ and $x_c/4$. Radial traverses were also made at $x = 32$ and $x = 0.2$ jet radii. These two locations were close to the limits of the measurement range set by the size of the LV optics and the dimensions of the working section window described in Sec. II.

Convergent and convergent-divergent nozzles were used in the subsonic and supersonic experiments, respectively. The correct operating conditions for ideal expansion for the convergent-divergent nozzles was determined using a shadowgraph technique.

Static pressure tappings were made in the working section wall to determine the wall static pressure gradient. It was found that the axial pressure gradient increased as the tunnel velocity increased. However, the gradient was very small and was equivalent to a variation of 2% in tunnel velocity in the working section at the highest tunnel velocity and 1% at the lowest tunnel velocity.

IV. Velocity Measurements

Centerline Traverses

The axial mean velocity on the jet centerline $\bar{u}_a/\bar{u}_J$, where $\bar{u}_J$ is the jet exit velocity for several velocity ratios and a jet exit Mach number of 0.47 is shown in Fig. 3. As the velocity ratio, λ, increases so the rate of decay of the jet centerline velocity decreases. The potential core length may also be seen to increase. Kleinstein[13] showed that an exact solution, for small radius, of the boundary-layer equations, based on an eddy viscosity that was a function of axial distance only, gave the centerline velocity, $\bar{u}_a$, in the form,

$$(\bar{u}_a/\bar{u}_J - \lambda)/(1-\lambda) = 1 - \exp\{-1/2\xi_v\} \tag{4}$$

ξ_v, which is a function of axial distance, was defined through the assumed eddy viscosity, and its numerical value was obtained from experimental centerline velocity measurements. For $M_J = 0.47$ the present measurements lead to a variation of ξ_v with λ and axial distance, x, of the form

$$\xi_v/r_J = 0.04(1 - 0.92\lambda)x/r_J - 0.35 \tag{5}$$

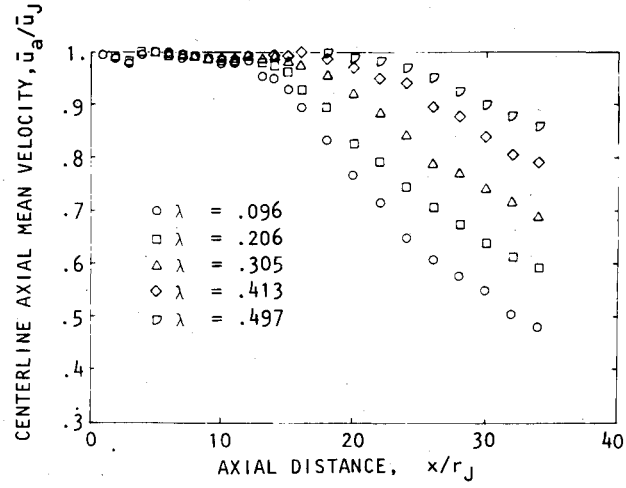

Fig. 3 Variation of axial mean velocity on the jet centerline with velocity ratio, $M_J = 0.47$.

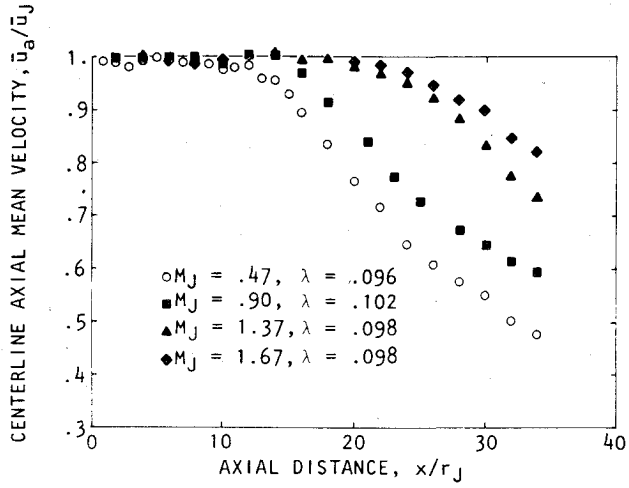

Fig. 4 Variation of axial mean velocity on jet centerline with Mach number, $\lambda = 0.1$.

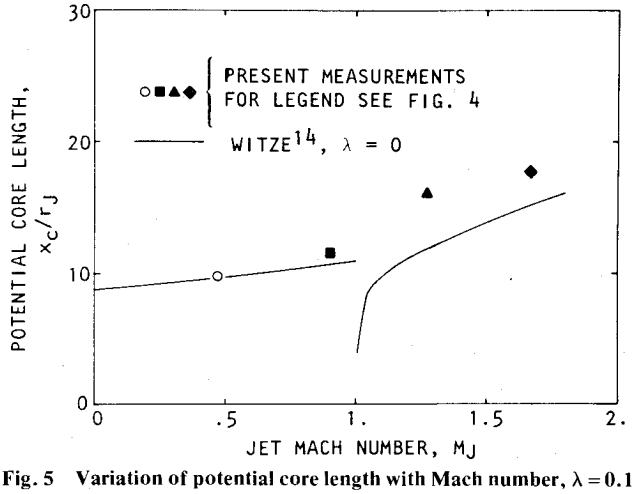

Fig. 5 Variation of potential core length with Mach number, $\lambda = 0.1$.

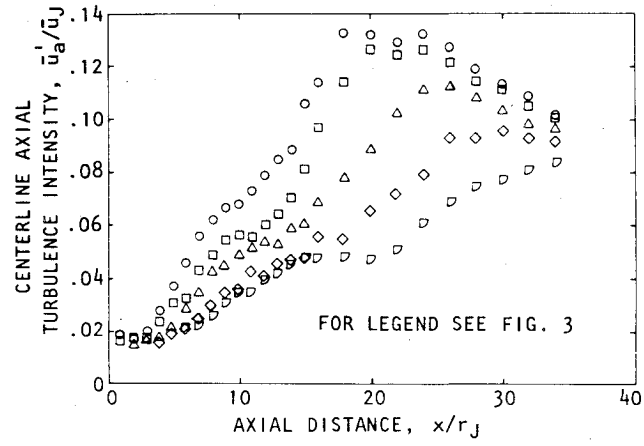

Fig. 6 Variation of axial turbulence intensity on the jet centerline with velocity ratio, $M_J = 0.47$.

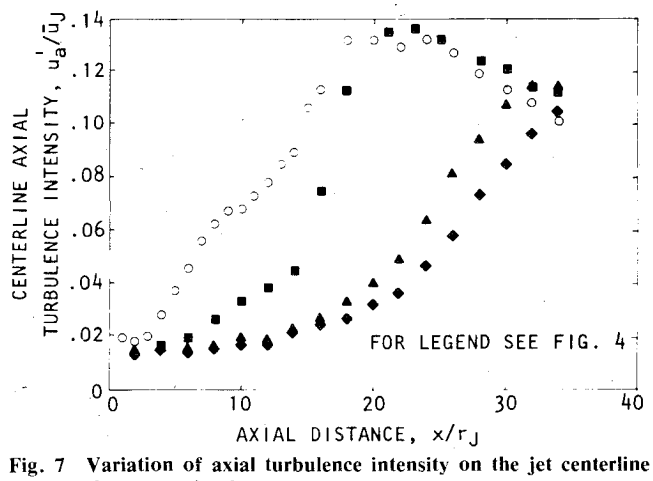

Fig. 7 Variation of axial turbulence intensity on the jet centerline with Mach number, $\lambda = 0.1$

This method of collapsing the centerline velocity data leads to a convenient nonarbitrary method of defining the potential core length. From Eqs. (4) and (5), the potential core length, x_c, is seen to be given by

$$x_c/r_J = 8.77/(1-0.92\lambda) \tag{6}$$

Forstall and Shapiro[7] predicted a linear increase of potential core length with velocity ratio (see Eq. (3) of this paper). However, Eq. (3) was obtained by fitting an expression of the form $(\bar{u}_a/\bar{u}_J - \lambda)/(1-\lambda) = x_c/x$ to the data, which does not fit the observation close to the end of the potential core, and leads to a slight overestimate of the potential core length.

It can be seen from Eq. (6) that the potential core length is finite even if the jet exit velocity and freestream velocity are equal. This represents the effects of boundary layers on the inner and outer walls of the nozzle and the finite lip thickness. In the absence of upstream boundary layers and for vanishingly small nozzle lip, Eq. (6) suggests a variation of potential core length with velocity ratio of the form,

$$x_c/r_J \propto (1-\lambda)^{-1} \tag{7}$$

The variation of the centerline velocity with Mach number for a fixed velocity ratio, $\lambda = 0.1$, is shown in Fig. 4. As the Mach number, M_J, increases so the rate of decay of the centerline velocity decreases. The potential core length increases with increasing Mach number. It should also be noted that the behavior of the mean velocity on the centerline is quite different for the subsonic and supersonic cases. This individual behavior of locally subsonic and supersonic flows also is apparent in the fluctuating velocity measurements and is discussed below.

The variation of potential core length with Mach number was calculated by fitting Eq. (4) to the measurements. The calculations are shown in Fig. 5. The measurements have been compared with the empirical correlation of Witze[14] for a velocity ratio of zero. The slight increase in core length with velocity ratio is more evident at the supersonic jet Mach number. However, the variation with jet Mach number is similar for both $\lambda = 0$ and $\lambda = 0.1$.

The variations of axial turbulence intensity on the jet axis, $u_a'/\bar{u}_J$, with velocity ratio and Mach number are shown in Figs. 6 and 7, respectively. The secondary peak, close to the jet exit, which is evident in all the $M_J = 0.47$ data, but is not seen at the higher Mach numbers, is caused by flow separation at an upstream valve leading to vortex-shedding from the jet lip. From Fig. 6, it can be seen that the peak axial turbulence intensity decreases with increase in velocity ratio, λ, and the location of the peak moves farther downstream. The difference between the centerline distributions of subsonic and supersonic jets which was evident in the axial mean velocity variation (Fig. 4) is also seen in the turbulence intensity distribution (Fig. 7). The empirical correlation of centerline velocity decay proposed by Witze[14] was based on a two-region model of the turbulent mixing process. This division of the flow into locally subsonic and supersonic regions appears sensible in the light of the present centerline traverses, although the transition is expected to be less abrupt than Witze's model. The peak turbulence intensity for the supersonic jets is lower than the subsonic peak value, and the location of the peak in the supersonic cases is further downstream.

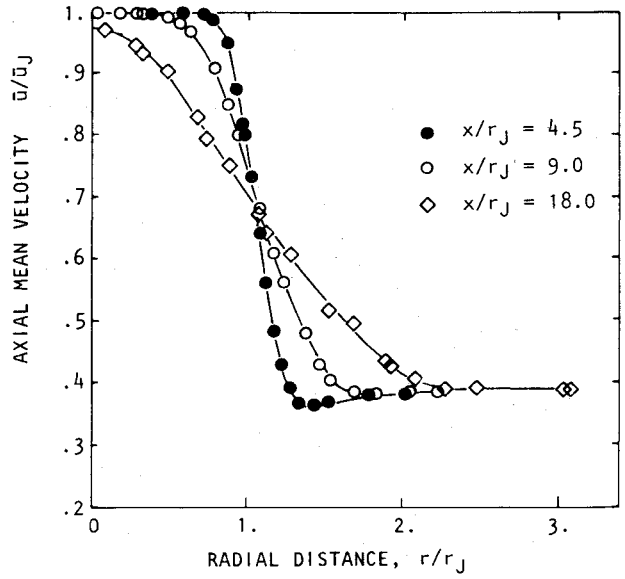

Fig. 8 Axial mean velocity profiles, $M_J = 0.47$, $\lambda = 0.4$.

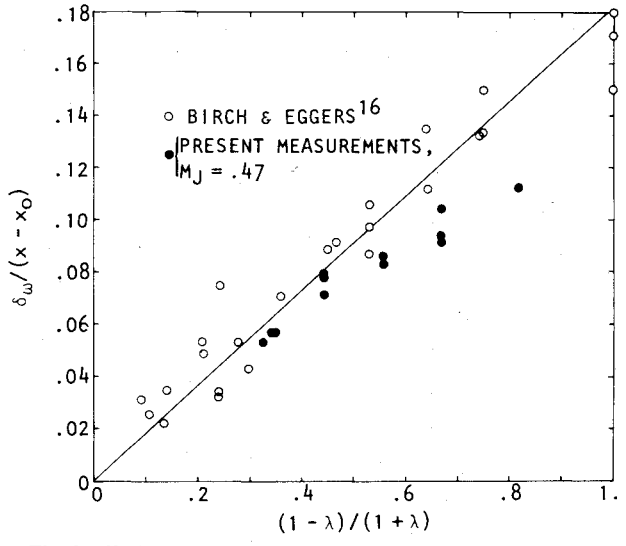

Fig. 9 Variation of spread rate with velocity ratio, $M_J = 0.47$.

Radial Traverses–Mean Velocity

A typical set of radial traverses of axial mean velocity for $M_J = 0.47$ and $\lambda = 0.4$ is shown in Fig. 8. The radial extent of the mixing region can be seen to increase with axial distance, and the centerline velocity has decreased at $x/r_J = 18$. The velocity profiles close to the jet exit exhibit a velocity defect close to the jet lip line showing that the effect of the initial boundary layers on the inner and outer surfaces of the jet nozzle still remains.

The mean velocity profiles are used to determine the variation of spreading rate of the jet with velocity ratio and Mach number. In the present investigation, the width of the jet is defined as the vorticity thickness, δ_ω, which is given by

$$\delta_\omega = (\bar{u}_a - \bar{u}_T)/(\partial\bar{u}/\partial r)_{\max} \tag{8}$$

Brown and Roshko[5] point out that this definition of thickness is appropriate, since the growth of the turbulent jet flow is primarily governed by the unstable motion induced by the vorticity. It has been found to be convenient to consider the jet in two separate regions: the annular mixing region up to the end of the potential core and the flow region downstream of the potential core. The results presented below concentrate on the annular mixing region. Measurements downstream of the potential core are discussed in Ref. 15.

It is to be expected that for sufficiently small ratios of vorticity thickness to potential core radius the initial mixing region will grow in the same manner as the two-dimensional mixing region. In fact, the spread rate of the axisymmetric jet is found to agree closely with that of the two-dimensional mixing region up to the end of the potential core. The variation of $\delta_\omega/(x-x_o)$ for present measurements in the annular mixing region and the variation for two-dimensional mixing layers, compiled by Birch and Eggers, [16] are compared in Fig. 9. x_o is the virtual origin of mixing found by assuming a linear variation of vorticity thickness with axial distance and finding the intercept on the jet axis. It can be seen that the variation of mixing region thickness with axial distance is similar for the two-dimensional and axisymmetric flows, although there is a tendency for the present results for a round jet to fall away from the two-dimensional mixing region results for small values of λ. A linear variation of vorticity thickness with $(1-\lambda)/(1+\lambda)$ is also shown in Fig. 9. The constant of proportionality used is 0.181; the value suggested by Brown and Roshko,[5] although a slightly lower value is indicated by the present measurements. The variation of δ_ω with λ may be shown to depend on the choice of a typical convection velocity for the turbulence.[5] A relationship of the form of Eq. (2) is based on a convection velocity of $(\bar{u}_1+\bar{u}_2)/2$, whereas, Eq. (1) uses a convection velocity of $(\bar{u}_1+\bar{u}_2)^{1/2}/2$. However, the scatter in the data, particularly at $\lambda = 0$, does not enable a definitive conclusion to be made as to the variation of spreading rate with velocity ratio.

When the vorticity thickness is used to normalize the radial distance, the mean velocity profiles in the annular mixing region may be collapsed. The mean velocity in the annular mixing region in the form $(\bar{u}-\bar{u}_T)/(\bar{u}_a-\bar{u}_T)$ is shown in Fig. 10 as a function of $(r-r_{0.5})/\delta_\omega$. $r_{0.5}$ is the half-velocity radius defined as the radial distance where $\bar{u} = (\bar{u}_a+\bar{u}_T)/2$. The variation of $r_{0.5}$ with axial distance in the mixing region is very slight, having a tendency to increase with axial distance at a rate that decreases with increasing velocity ratio. Although $\bar{u}_a/\bar{u}_J$ is equal to unity in most cases, some data just downstream of the end of the potential core have been included. Mean velocity profiles that occur in the region of the flow establishment, where the wake velocity defect downstream of the jet lip still exists, have not been included. The collapse is seen to be very good. A reasonable fit to the data is given by the expression

$$(\bar{u}-\bar{u}_T)/(\bar{u}_a-\bar{u}_T) = 0.5(1-\sin 2\eta) \qquad -\pi/4 \le \eta \le \pi/4 \tag{9}$$

where $\eta = (r-r_{0.5})/\delta_\omega$. The simple expression (9) has a derivative of -1 at $\eta = 0$. This is consistent with the choice of δ_ω as the characteristic length as the collapsed profiles then have a slope of -1 at the point of maximum shear, which occurs close to the half-velocity radius in the annular mixing region.

The effect of change in jet Mach number for a fixed velocity ratio is now examined. Brown and Roshko[5] used an order of magnitude analysis to suggest a dependence of the spreading rate, $d\delta_\omega/dx$, on Mach number. For sufficiently high Mach numbers, the spread rate was found to be inversely proportional to the Mach number. In Fig. 11 the present measurements of $d\delta_\omega/dx$ for several jet Mach numbers and a velocity ratio $\lambda = 0.1$ are compared with the data compiled by Birch and Eggers.[16] Both sets of data suggest an inverse Mach number dependence for the supersonic cases. For $\lambda = 0$ the subsonic data suggests little variation of spreading rate with Mach number. Until further data is available, it may be concluded that the dependence of jet width on velocity and Mach number is well represented by

$$d\delta_\omega/dx \propto (1-\lambda)((1+\lambda) \qquad M_J < 1$$

$$d\delta_\omega/dx \propto (1-\lambda)/(1+\lambda)M_J^{-1} \qquad M_J > 1 \tag{10}$$

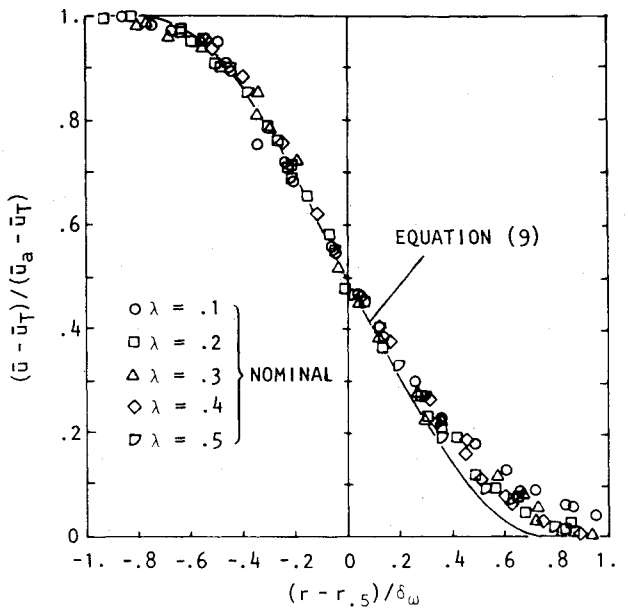

Fig. 10 Radial distribution of axial mean velocity in the annular mixing region for various velocity ratios.

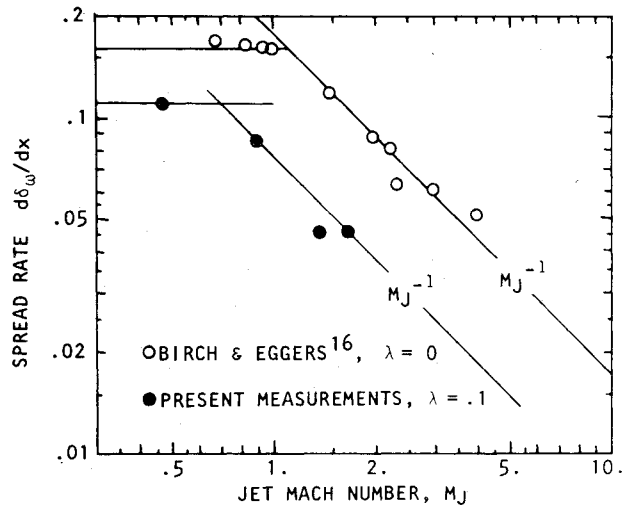

Fig. 11 Variation of spread rate with Mach number, $\lambda = 0.1, 0$.

Radial Traverses-Turbulence Intensity

Since the peak axial turbulence intensity is shown to be a function of velocity ratio and was also found to decrease slightly with axial distance in the annular mixing region, the radial distributions of turbulence intensity will be normalized with respect to their maximum value. The normalized turbulence intensity distributions, u'/u'_{max}, for a fixed jet exit Mach number, $M_J = 0.47$, and several velocity ratios is shown in Fig. 12. The data collapse well for all the velocity ratios, and the location of the peak turbulence intensity occurs close to the half-velocity radius. The data of Davies[17] for the mixing region of a free jet, $\lambda = 0$, are shown for comparison, and the agreement is good.

The normalized turbulence intensity distributions, in the annular mixing region for $\lambda = 0.1$ for several jet exit Mach numbers are shown in Fig. 13. The data for subsonic and supersonic jet exit velocities have similar distributions near the center of the mixing layer, $(r - r_{0.5})/\delta_\omega = 0$, although there is a tendency for the turbulence intensity to fall less rapidly with radial distance in the outer region of the jet for the supersonic jet exit velocities. This slight change in turbulent structure from subsonic to supersonic conditions was observed in the axial distributions of mean velocity and turbulence intensity shown in Fig. 4 and 7, respectively. Since the jets were carefully run at the ideally expanded operating conditions, it is unlikely that these differences may be explained by the influence of any weak shock structure.

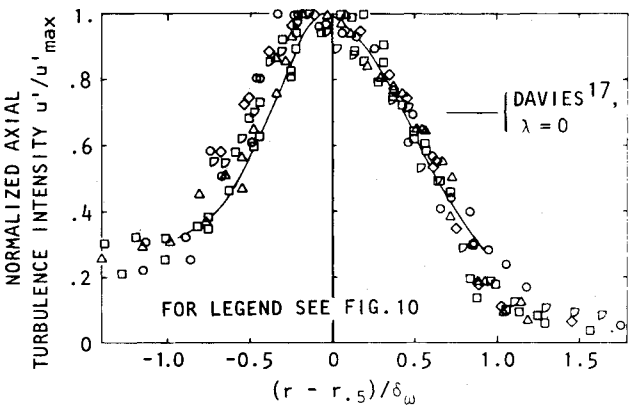

Fig. 12 Radial distribution of axial turbulence intensity in the annular mixing region for various velocity ratios, $M_J = 0.47$.

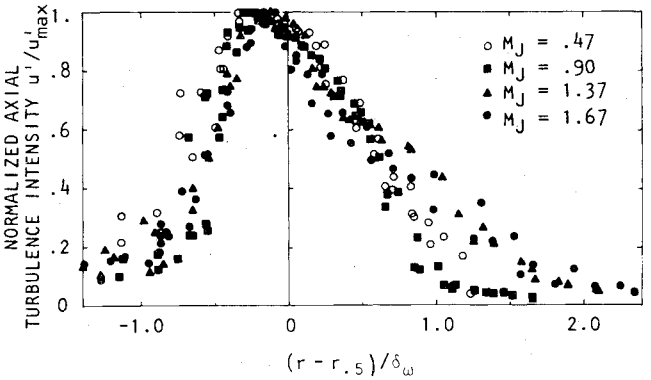

Fig. 13 Radial distribution of axial turbulence intensity in the annular mixing region for various Mach numbers, $\lambda = 0.1$.

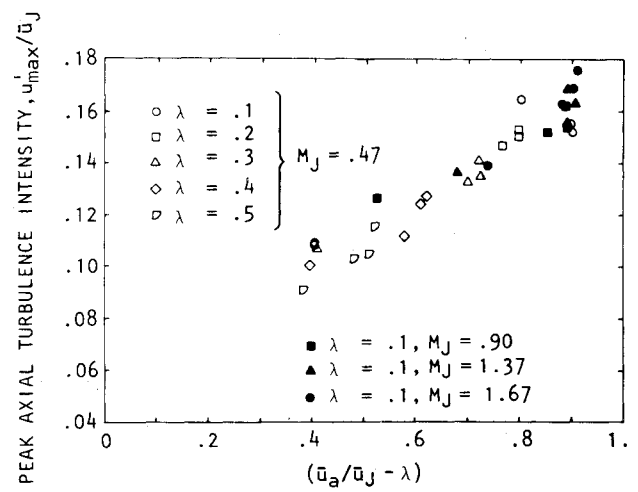

Fig. 14 Variation of peak axial turbulence intensity with velocity difference, $(\bar{u}_a/\bar{u}_J - \lambda)$, for various velocity ratios and Mach numbers.

The variation of the peak axial turbulence intensity, $u'_{max}/\bar{u}_j$, with normalized velocity difference, $(\bar{u}_a/\bar{u}_j - \lambda)$, is shown in Fig. 14 for both subsonic and supersonic jet exit velocities. Although, there is a tendency for the peak axial turbulence intensity to increase with Mach number, the change is very small and is within experimental error at these higher velocities. The apparent linear increase of $u'_{max}/\bar{u}_J$ with normalized velocity difference suggests an expression of the form

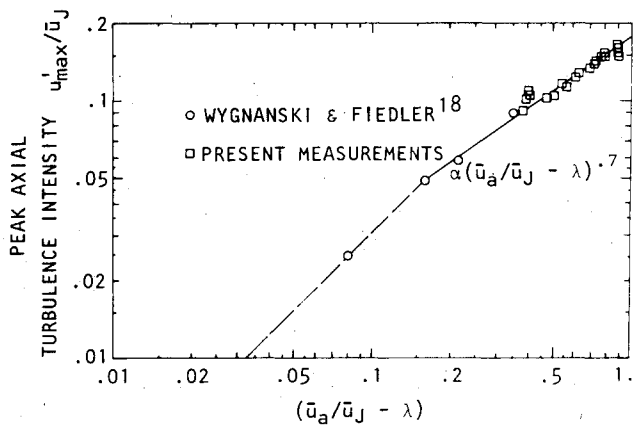

Fig. 15 Variation of peak axial turbulence intensity with velocity difference.

$$u'_{max}/\bar{u}_J = A + B(\bar{u}_a/\bar{u}_J - \lambda) \tag{11}$$

The value of A, found by a linear least squares fit, of 0.051, would appear to properly account for the initial boundary layers since $\bar{u}_a/\bar{u}_J$ equal to λ gives an axisymmetric wake flow close to the jet exit. However, the expression is not reasonable further downstream, when $\bar{u}_a/\bar{u}_J$ tends to λ, since it leads to a maximum turbulence intensity that scales with jet exit velocity. It is more reasonable to assume that close to the jet exit the turbulence intensity scales with difference between the centerline velocity and the minimum axial velocity which would occur close to the lip line in the region of flow establishment. No measurements were made in the present experiments for small velocity differences. However, for the case of an axisymmetric jet, the variation of $u'_{max}/\bar{u}_J$ with normalized velocity difference for small velocity differences can be inferred from measurements of axisymmetric jets into still air far downstream of the jet exit where the jet centerline velocity is very small. The measurements by Wyganski and Fiedler[18] show that by 40 diam downstream of the jet exit the value of u'_{max} is a constant fraction of the centerline velocity, namely

$$u'_{max}/\bar{u}_J = 0.3(\bar{u}_a/\bar{u}_J - \lambda) \qquad (\bar{u}_a/\bar{u}_J - \lambda) < 0.163 \tag{12}$$

In Fig. 15, Wyganski and Fiedler's and the present measurements of $u'_{max}/\bar{u}_J$ have been plotted as a function of $(\bar{u}_a/\bar{u}_J - \lambda)$. The variation can be divided into two regions. The first is given by Eq. (12) and the second is given by

$$u'_{max}/\bar{u}_J = 0.175(\bar{u}_a/\bar{u}_J - \lambda)^{0.7} \qquad (\bar{u}_a/\bar{u}_J - \lambda) > 0.163 \tag{13}$$

The slope of the linear portion of the curve, Eq. (12) and hence the crossover between the two curves will be a function of the wake-generating body. Various asymptotic values of $u'_{max}/(\bar{u}_a - \bar{u}_T)$ have been noted by Antonia and Bilger.[6] The nonlinear dependence of u'_{max} on velocity difference given by Eq. (13), shows how the influence of the jet exit velocity, which governs the mixing in the inner region of the jet especially the initial mixing layer, persists far downstream of the jet exit. If it were not for this persistent influence of upstream conditions on the local flow structure, the turbulence would be expected to always scale linearly with velocity difference. The exponent 0.7 in Eq. (13) is thus seen as being dependent on the initial conditions in the present experiments. However, unless the initial boundary layers are removed and the jet lip is made vanishingly small, this empirical exponent should be typical of most realistic experimental configurations.

Radial Traverses–Skewness and Kurtosis

The nth central moment, μ_n, of the velocity probability distribution function, $f(u)$, is defined by

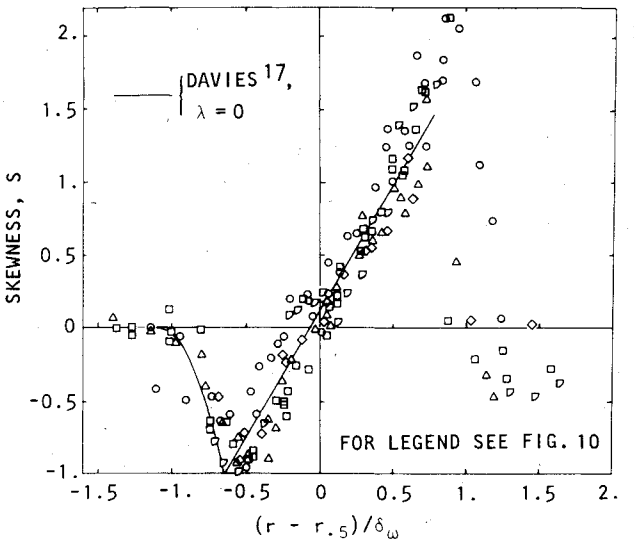

Fig. 16 Radial distribution of skewness of the axial velocity in the annular mixing region for various velocity ratios, $M_J = 0.47$.

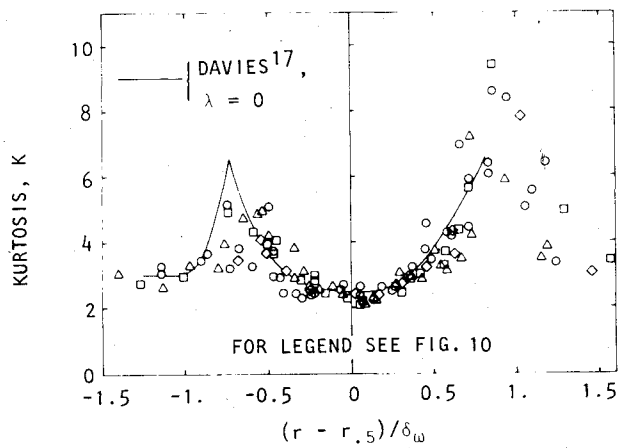

Fig. 17 Radial distribution of kurtosis of the axial velocity in the annular mixing region for various velocity ratios, $M_J = 0.47$.

$$\mu_n = \int_{-\infty}^{\infty} (u - \bar{u}) f(u)\, du \tag{14}$$

where $\bar{u}$ is the mean velocity. The normalized third and fourth probability moments are called the skewness, S, and the kurtosis or flatness factor, K, respectively. The normalization is such that,

$$S = \mu_3/(\mu_2)^{3/2} \text{ and } K = \mu_4/(\mu_2)^2 \tag{15}$$

noting that μ_2, the second central moment, is the mean square velocity. The radial distributions of skewness and kurtosis in the annular mixing region for fixed jet exit Mach number $M_J = 0.47$, and several velocity ratios λ are plotted as functions of $(r - r_{0.5})/\delta_\omega$ in Figs. 16 and 17, respectively. The data collapse well and agree with the best fit of Davies[17] for a free axisymmetric jet, $\lambda = 0$. At the inner edge of the mixing region, the velocity probability distribution is Gaussian being unskewed and having kurtosis of 3. Close to half-velocity point, the probability distribution is again unskewed but is no longer Gaussian. The probability distribution is negatively skewed on the inner side of the mixing layer and positively skewed on the outer side. Associated with the skewed signals are peaks in the kurtosis, the peak value being greater in the outer region. A feature of the velocity probability distribution, not evident from the free jet, $\lambda = 0$, data is its return to a Gaussian form at the outer boundary of the jet.

The positive and negative skewness and the kurtosis peaks are associated with the occurence of spikes in the velocity time history. Lau and Fisher[19] associated these spikes with bursts of high- and low-velocity fluid induced, from the inner and outer regions of the flow, respectively, by the passage of a well-ordered vortex structure.

V. Summary and Conclusions

Velocity measurements of a turbulent jet in a moving stream have been made for both subsonic and supersonic jet exit velocities using a single-channel backscatter laser velocimeter. Increasing the velocity ratio for fixed jet Mach number or increasing the jet exit Mach number for a fixed velocity ratio has been shown to decrease the axial rate of development of the jet flow. This results in a lowering of the spread rate and an increase in the potential core length with the associated axial displacement of the peak in the centerline axial turbulence intensity. Increasing the velocity ratio also results in a decrease in the peak axial turbulence intensity. However, this peak intensity does not scale with the velocity difference across the shear layer in the annular mixing region. This is the result of the domination of the flow structure by the shear layer shed from the inside of the jet lip, which has an initial velocity difference given by the exit velocity.

Although the secondary stream has been shown to have a considerable effect on the absolute scales of the jet, little effect is seen on the turbulent mixing structure. This has been shown from the skewness and kurtosis distributions. These factors are obtained by normalizing the higher order probability moments with respect to appropriate powers of the second order moment or mean square velocity fluctuation. It has been noted that the characteristics of the velocity probability distribution may be related to a particular turbulent structure. Since the radial distributions of skewness and kurtosis are not affected by variation in velocity ratio, it may be concluded that the turbulent structure or the mixing process is independent of the velocity ratio.

References

[1] Yule, A. J., "On the Mixing of Two Parallel Streams," Ph.D. Thesis, University of Manchester, Manchester, England, 1970.

[2] Görtler, H., "Berechnung von Aufgaben der Freien Turbulenz auf Grund eines Neuen Naherungsanstazes," *Zeitschrift für Angewandte Mathematik und Mechanik*, Vol. 22, Pt. 5, 1942, pp. 244–254.

[3] Miles, J. B., and Shih, J. S., "Similarity Parameter for Two-Stream Turbulent Jet Mixing Region," *AIAA Journal*, Vol. 6, July 1968, pp. 1429–1430.

[4] Sabin, C. M., "An Analytical and Experimental Study of the Plane, Incompressible, Turbulent Free Shear Layer with Arbitrary Velocity Ratio and Pressure Gradient," Dept. of Mechanical Engineering, Stanford University, Stanford, Calif., MD-9, 1963.

[5] Brown, G. L. and Roshko, A., "On Density Effects and Large Structure in Turbulent Mixing Layers," *Journal of Fluid Mechanics*, Vol. 64, 1974, Pt. 4, pp. 775–816.

[6] Antonia, R. A., and Bilger, R. W., "An Experimental Investigation of an Axisymmetric Jet in a Co-Flowing Airstream," *Journal of Fluid Mechanics*, Vol. 61, 1973, Pt. 4, pp. 805–822.

[7] Forstall, W. and Shapiro, A. H., "Momentum and Mass Transfer in Coaxial Gas Jets," *Journal of Applied Mechanics*, Vol. 17, No. 4, 1950, pp. 399–408.

[8] Whiffen, M. C., and Meadows, D. M., "Two-Axis Single Particle Laser Velocimeter System for Turbulence Spectral Analysis," March 1972, Laser Doppler Velocimeter Workshop, Purdue University, West Lafayette, Ind.

[9] Smith, D. M. and Meadows, D. M., "Power Spectra from Random-Time Samples for Turbulence Measurements with a Laser Velocimeter," March 1972, Laser Doppler Velocimeter Workshop, Purdue University, West Lafayette, Ind.

[10] Yanta, W. J., "Turbulence Measurements with a Laser Doppler Velocimeter," Naval Ordinance Lab. Md., NOLTR 73-94, 1973.

[11] Cline, V. A., and Bentley, H. T., "Application of a Dual-Beam Laser Velocimeter to Turbulent Flow Measurements. Arnold Engineering and Development Center, Tenn., 1974.

[12] McLaughlin, D.K. and Tiederman, W.G., "Biasing Correction for Individual Realization Laser Anemometer Measurements in Turbulent Flows, *Physics of Fluids*, Vol. 16, No. 12, 1973, pp. 2082–2088.

[13] Kleinstein, G., "Mixing in Turbulent Axially Symmetric Free Jets," *Journal of Spacecraft*, Vol. 1, April 1964, pp. 403–408.

[14] Witze, P. O. "Centerline Velocity Decay of Compressible Free Jets," *AIAA Journal*, Vol. 12, April 1974, pp. 417–418.

[15] Morris, P. J. "Turbulence Measurements in Subsonic and Supersonic Axisymmetric Jets in a Moving Stream," AIAA Paper 76-25, 1976, Washington D. C.

[16] Birch, S. F., and Eggers, J. M., "A Critical Review of the Experimental Data for Developed Turbulent Free Shear Layers," *Proceedings of the NASA Conference on Free Turbulent Shear Flows*, Vol. 1, NASA SP-321, 1972, pp. 11–37.

[17] Davies, P. O. A. L., "Turbulence Structure in Free Shear Layers," *AIAA Journal*, Vol. 4, Nov., 1966, pp. 1971–1978.

[18] Wygnanski, I. and Fiedler, H., "Some Measurements in the Self-Preserving Jet," *Journal of Fluid Mechanics*, Vol. 38, No. 3, 1969, pp. 577–612.

[19] Lau, J. C., and Fisher, M. J., "The Vortex-Sheet Structure of 'Turbulent' Jets. Part I." *Journal of Fluid Mechanics*, Vol. 67, Pt. 2, 1975, pp. 299–337.